Materials Science & Engineering C 115 (2020) 111009

Contents lists available at ScienceDirect

Materials Science & Engineering C

journal homepage: www.elsevier.com/locate/msec

Alginate-hydrogel versus alginate-solid system. Efficacy in bone regeneration in osteoporosis

Patricia García-García[a], Ricardo Reyes[b,d], Edgar Pérez-Herrero[a,d], María Rosa Arnau[c,d], Carmen Évora[a,d,*], Araceli Delgado[a,d,*]

[a] Department of Chemical Engineering and Pharmaceutical Technology, Universidad de La Laguna, 38200 La Laguna, Spain
[b] Department of Biochemistry, Microbiology, Cell Biology and Genetics, Universidad de La Laguna, 38200 La Laguna, Spain
[c] Servicio de Estabulario, Universidad de La Laguna, 38200 La Laguna, Spain
[d] Institute of Biomedical Technologies (ITB), Center for Biomedical Research of the Canary Islands (CIBICAN), Universidad de La Laguna, 38200 La Laguna, Spain

ARTICLE INFO

Keywords:
Scaffold
BMP-2
β-Estradiol
Osteoporosis
Bone regeneration
Mesenchymal stem cells

ABSTRACT

In the present study, two different PLGA-Alginate scaffolds, a hydrogel (HY) and a solid sponge (SS), were developed for β-estradiol and BMP-2 sustained delivery for bone regeneration in osteoporosis. β-Estradiol and BMP-2 were encapsulated in PLGA and PLGA-Alginate microspheres respectively. Scaffolds were characterized in vitro in terms of porosity, water uptake, release rate and HY rheological properties. BMP-2 release profiles were also analysed in vivo. The bone regeneration induced by both HY and SS was evaluated using a critical-sized bone defect in an osteoporotic (OP) rat model. Compared to HY, SS presented 30% higher porosity, more than double water absorption capacity and almost negligible mass loss compared to the 40% of HY. Both systems were flexible and fit well the defect shape, however, HY has the advantage of being injectable. Despite both delivery systems had similar composition and release profile, bone repair was around 30% higher with SS than with HY, possibly due to its longer residence time at the defect site. The incorporation of mesenchymal stem cells obtained from OP rats did not result in any improvement or synergistic effect on bone repair.

1. Introduction

The regeneration of the bone mass lost by several causes such as trauma, infections or surgery requires the contribution of three key elements: scaffolds, cells and growth factors [1–3]. Scaffolds are porous structures able to adapt to the bone defect acting as support and guide for cell proliferation and differentiation with the help of signalling molecules [4,5]. Therefore, scaffolds must also act as reservoirs for growth factors involved in the cascade of cellular events that leads to bone formation.

Clearly, the best bone graft is autologous bone, however, several well-known disadvantages (invasive surgery, limited availability and damage in the donor bone) have led to the search for alternative approaches [6]. The type of biomaterials used to develop scaffolds for bone regeneration during the last decades is very wide. Taking into account the scaffolds active role in bone regeneration as artificial extracellular matrix, different biodegradable and/or osteointegrable materials of diverse nature (phosphates, bio-glass, natural and synthetic polymers) have been used to construct 3D-scaffolds. The design of these scaffolds is based on fulfilling several characteristics to facilitate tissue ingrowth, such as biocompatibility, porous structure with interconnected pores, permeability for blood perfusion, nutrients supply, cell adhesion and differentiation [7]. Hydrogels suit these characteristics, thus the development and preparation of biodegradable hydrogels for bone tissue engineering applications is currently of great interest [8,9]. In addition, scaffold bioactivity is required to successfully tackle critical size bone defect regeneration. One strategy to “activate” scaffolds is their loading with growth factors such as bone morphogenetic proteins (BMPs). Particularly, BMP-2, which is involved in most of the processes required for bone formation [1,6]. In fact, due to its osteogenic capacity rhBMP-2 is already marketed incorporated in a collagen scaffold to locally treat some bone injuries [10]. The benefits of rhBMP-2 have been already proven nevertheless, the risk of adverse effects associated with the high dose required in the clinic and the inability of the carrier to retain the protein in the defect, make necessary the development of scaffolds with controlled release capacity for greater efficacy and safety [10]. Injectability and adaptability to the bone defect shape are among the most characteristic advantages of hydrogels [8,9]. However, their weak mechanical properties and short residence time in the defect could be a disadvantage depending on the

* Corresponding authors at: Department of Chemical Engineering and Pharmaceutical Technology, Universidad de La Laguna, 38200 La Laguna, Spain.
E-mail addresses: cevora@ull.edu.es (C. Évora), adelgado@ull.edu.es (A. Delgado).

https://doi.org/10.1016/j.msec.2020.111009
Received 22 November 2019; Received in revised form 1 April 2020; Accepted 21 April 2020
Available online 23 April 2020

type of bone lesion to be treated. Finally, their incapacity to regulate growth factors release has led to the development of different strategies to control drug release rate by increasing the drug binding to the hydrogel matrix [11–13] or combining hydrogels with sustained release platforms [12–14]. We previously reported hydrogels composed of poloxamine alone or combined with alginate or cyclodextrin containing microspheres of different composition to control BMP-2 release. These systems were tested in osteoporotic (OP) and non-OP rats, not observing significant differences in bone repair between both groups [15–18]. However, the mineralization in OP groups was notably inferior to that of non-OP groups [17,18]. Given that all bone repair processes are impaired and bone healing time is delayed in OP [19–22], to overcome the low mineralization observed in our previous study we hypothesized a longer residence time of the scaffold in the defect and a longer release of BMP-2 in OP is required.

In this study, a new alginate hydrogel system, crosslinked in two steps and loaded with β-estradiol and BMP-2 within microspheres was developed. Microspheres were elaborated from a combination of alginate and polylactide-*co*-glycolide (PLGA) with different lactide to glycolide ratio and molecular weight (Mw). The hydrogel system was compared with a solid sponge system with the same composition. The goal is to keep similar some of the physical and chemical properties for both systems such as composition, hydrophilicity/hydrophobicity, water uptake, swelling behaviour and porosity and BMP-2 and β-estradiol release rates. The main expected difference between both systems is the scaffold residence time in the critical size calvarial defect. Therefore, two β-estradiol-BMP-2-Alginate-PLGA systems, hydrogel (HY) and solid sponge (SS), were developed and in vitro characterized. The induced bone regeneration by both systems was compared in a critical size defect in OP rats alone or seeded with OP mesenchymal stem cells (MSCs).

2. Materials and methods

2.1. Materials

The polylactide-*co*-glycolide 75:25 (PLGA 75:25, Resomer® RG 755 S) and 85:15 (PLGA 85:15, Resomer® RG 858 S) and the sodium alginate (Protasan® UP MVG) were supplied by Evonic Industries (Darmstadt, Germany) and Novamatrix (Biopolymer Systems, Sandvika, Norway) respectively. 17-β-estradiol and recombinant human bone morphogenetic protein 2 (rhBMP-2) were purchase from Sigma-Aldrich (USA) and Biomedal Life Sciences (Sevilla, Spain) respectively. rhBMP-2 was reconstituted at 1 mg/mL in 20 mM acetic acid and 0.1% bovine serum albumin (BSA, Sigma-Aldrich, St. Louis, USA). Poly(vinyl alcohol) (PVA, Mw 33,000-70,000; 87–90% hydrolysed) was from Sigma-Aldrich, (St. Louis, USA) and $CaCl_2$ from Merck (Darmstadt, Germany).

2.2. Microsphere preparation and characterization

The alginate-PLGA microspheres of BMP-2 were prepared by modifying a previously described double emulsion (w/o/w) method [23,24]. Briefly, an aqueous solution of 500 μL of rhBMP-2 (500 μg), 100 μL of 15% polyvinyl alcohol (PVA) and 300 μL of 6% sodium alginate (*w/v*) was emulsified with 2 mL of a mixture of PLGA 75:25 and PLGA 85:15 (4:1) methylene chloride solution (125 mg/mL, DCM) by vortexing (position 10, Genie® Industries 2, Sciencies Industries Inc. USA) for 1 min. Then, 5.2 mL of an aqueous solution of 2.5 mL of PVA (10% *w/v*), 2.5 mL of NaCl (10% w/v) and 200 μL of $CaCl_2$ (0.5 M) was poured over the first emulsion and vortexed for 30 s (position 10). Finally, the organic solvent was evaporated in 100 mL of 0.25 M $CaCl_2$ aqueous solution under constant magnetic stirring for 1.5 h.

The microspheres of β-estradiol were prepared by the solvent evaporation method. Briefly a mixture of β-estradiol (6 mg), PLGA 75:25 (160 mg) and PLGA 85:15 (40 mg) dissolved in 0.6 mL methanol:DCM (20:80) solution was emulsified with 4 mL of 1% PVA aqueous solution by vortexing for 1 min (position 10), poured into 100 mL of PVA (0.15%) aqueous solution and left under magnetic stirring for 1 h [17,18].

Both types of microspheres were collected by filtration (Supor®-450, 0.45 μm, 47 mm filters, Pall Corporation, Sigma-Aldrich, USA), lyophilized and conserved at 4 °C until use.

Some batches were prepared with ^{125}I-BMP-2 as a tracer to determine rhBMP-2 encapsulation efficiency and release assays. BMP-2 was labelled with ^{125}INa (Perkin-Elmer) by the iodogen method [25], as described [16]. The content of β-estradiol in the microspheres was determined spectrophotometrically at λ = 280 nm, previous dissolution in a mix of MeOH:DCM (20:80).

Microspheres size distribution was determined by laser diffractometry using a Mastersizer 2000 (Malvern Instruments, Malvern, UK) and the morphology was observed by scanning electron microscopy (SEM, Jeol JSM-6300, Tokio, Japan).

2.3. Fabrication and characterization of electrospinning film

The polymer film was fabricated by electrospinning a solution of PLGA 75:25 and PLGA 85:15 at a ratio 4:1 and β-estradiol. Briefly, 7 mg of β-estradiol, 240 mg of PLGA 75:25 and 60 mg of PLGA 85:15 dissolved in 2 mL of hexafluoroisopropanol (Sigma-Aldrich, USA) were loaded into a Luer-lock syringe (Norm-Ject) with an 18-gauge needle attached to a syringe pump (Harvard Apparatus, MA, USA). The electrospinning process was carried out at a flow rate of 3 mL/h under 10 kV power supply and the collector rotating at 200 rpm located at 10 cm from the needle.

The film quality and fiber diameter were analysed using SEM (Jeol, JSM-6300) images and the film thickness was measured by stereo microscopy (Leica M205C, Leica Las, v 3 software).

The porosity was calculated using Eq. (1), where ρ_{app} and ρ_{real} are the apparent and real densities of the film, respectively,

$$\text{Porosity}\ (\%) = \left(\frac{\rho_{real} - \rho_{app}}{\rho_{real}}\right) \times 100 \quad (1)$$

The real density was measured in a helium pycnometer (AccuPyc 1330, Micromeritics, USA). While the real density was calculated by dividing the mass by the geometric volume of the film (length × width × height).

Water uptake and mass loss assays were carried out by samples (3 × 3 cm) incubation in water (37 °C) under orbital agitation (25 rpm). At specific times, three samples were withdrawn, the excess of water removed, weighted and freeze-dried to record the dry weight. The percentages of mass loss and water uptake were calculated applying Eqs. (2) and (3), respectively. Where W_o was the initial weight of the sample, W_w and W_d were the weights of the wet and dried sample respectively, at the different times tested.

$$\text{Mass loss}\ (\%) = \frac{(W_0 - W_d)}{W_0} \times 100 \quad (2)$$

$$\text{Water uptake}\ (\%) = \frac{(W_w - W_d)}{W_d} \times 100 \quad (3)$$

2.4. Systems preparation and characterization

2.4.1. Solid system

To prepare the alginate solid sponge system 15 mg of microspheres were dispersed in 100 μL of 2% alginate aqueous solution and freeze-dried. The alginate was then cross-linked by incubation with 100 μL of 1% $CaCl_2$ during 3 min and washed with 100 μL of sterile MilliQ water three times and freeze-dried. All the systems were stored at 4 °C until use.

2.4.2. Hydrogel system

To prepare the alginate hydrogel system 4.5% *w*/w sodium alginate sterile aqueous solution was partially cross-linked by sufficient quantity of a 1% w/w $CaCl_2$ sterile aqueous solution to give final concentrations of 4% w/w of sodium alginate and 0.12% w/w of $CaCl_2$. Then, 15 mg of microspheres were dispersed in the partially cross-linked hydrogel (PC-HY). Afterward, it was cross-linked with 5% w/w $CaCl_2$ sterile aqueous solution (0.7 μL/μL of hydrogel).

The systems were characterized in terms of porosity, water uptake and mass loss, as previously described for the polymer film (Eqs. (1), (2) and (3)). Morphology and structural characteristics were observed by SEM (Jeol JSM-6300). For hydrogel characterization, the system was prepared in a graduated cylindrical mold and freeze-dried.

In addition, rheological characteristics of the PC-HY, freshly prepared with and without microspheres, and after 4 h at rest (PC-HY + 4 h), were obtained with a Bohlin CVOD 100 rheometer at 20 °C and 37 °C by means of a Peltier system, using cone-plate and parallel geometries with a diameter of the fixed lower plate of 60 mm and a gap between the fixed and rotating part of 1 mm. The evolution of viscosity with shear rate (from 0.071 to 30 s^{-1}) was acquired by a cone-plate geometry (diameter of cone 40 mm, angle 4°). The evolution of elastic (G′) and viscous moduli (G″) with frequency (0.128 a 6.93 Hz) was acquired by a parallel plate geometry (diameter of rotating upper plate 20 mm) at a constant shear stress of 0.2387 Pa.

The systems to be implanted were prepared under aseptic conditions and all contained 6 μg of BMP-2 in microspheres. In addition, the solid sponge systems were loaded with 300 μg of β-estradiol in microspheres (SS-BMPβe). However, in the hydrogel system the dose of β-estradiol was divided, 240 μg in microspheres dispersed in the hydrogel and placed in between two electrospun films containing 60 μg of β-estradiol forming an alginate hydrogel sandwich system (HY-BMPβe). Both systems, solid sponge and hydrogel, seeded with MSCs obtained from osteoporotic rats, SS-BMPβe-MSC and HY-BMPβe-MSC, were also implanted.

2.5. In vitro release assay

The rhBMP-2 in vitro release assays were carried out by incubating (37 °C, 25 rpm orbital stirring) each system in sterile water (Milli-Q). The amount of the ^{125}I-BMP-2 released was calculated by measuring the radioactivity of supernatant samples (Cobra® II, Packard).

The in vitro release assays of β-estradiol from free microspheres, microspheres in the HY, microspheres in the SS and samples of the electrospun films were carried out in three release media (37 °C, 25 rpm orbital stirring), dimethyl sulfoxide (DMSO, Acofarma, Barcelona, Spain):H_2O (40:60), MeOH:H_2O (50:50) and sodium lauryl sulphate (SLS, Sigma-Aldrich, St. Louis, USA) in water (1% *w/v*).

2.6. Cells

Bone marrow rat MSCs were obtained as described [26] from femur and tibiae bone marrow of 18 weeks-old female Sprague-Dawley rats ovariectomized (OVX) 12 weeks before. Briefly, whole bone marrow was pooled and resuspended in Dulbecco's Minimal Essential Medium (DMEM) with 4.5 g/L glucose, supplemented with 20% fetal bovine serum, 50 UI/mL penicillin, 50 μg/mL streptomycin, and 200 mM stabilized L-glutamine, seeded on cell culture plastic, and incubated at 37 °C and 5% CO_2. After 3 days, non-adhered cells were removed and fresh medium was added. Confluent cells were detached and frozen. Stock frozen MSCs were thawed, precultured for 3–4 d, and trypsin-detached for scaffold loading. The SS-BMPβe-MSC and HY-BMPβe-MSC systems were loaded with 5×10^5 MSCs in passage 2 suspension (60 μL) approximately 20 min before implantation.

The 60 μL of the MSCs suspension were dropped on the solid sponge or mixed with the microspheres in the hydrogel system. In previous in vitro studies it was demonstrated that both the materials used and the type of scaffolds are biocompatible with MSCs, allowing their adhesion and viability [27,28].

2.7. Animals experiments

All animal experiments were carried out in conformity with the European Directive (2010/63UE) on Care and Use of Animals in Experimental Procedures. Furthermore, the animal protocols (CEIBA2014-0128) were approved by the ethics committee for animal care of the University of La Laguna. Animals were supplied by the Central Animal House of the University of La Laguna.

2.7.1. Surgical procedures

30 female Sprague-Dawley rats, weighing 250–300 g, were used in this study. Surgery was made under aseptic conditions. The experimental osteoporosis was induced by bilateral ovariectomy (OVX) under isoflurane anaesthesia, via dorsal approach. Three months post-OVX, critical size (8 mm, ∅) calvarial defects were created surgically with a trephine burr in the rats under isoflurane and the systems were placed into the defects, as previously described [29]. Analgesia consisted in buprenorphine administered subcutaneously (0.05 mg/kg) before surgery and paracetamol (70 mg/100 mL) in the water for 3 days post-surgery.

2.7.2. Animal groups

The 30 female rats pre-OVX were dividing in 6 groups of 5 rats each. 2 groups of 5 OP rats each were implanted with SS-^{125}I-BMPβe and HY-^{125}I-BMPβe to determine the ^{125}I-BMP-2 release kinetics. After 6 weeks the rats were sacrificed.

The other four groups were used to evaluate bone regeneration induced by a combination of BMP-2 and β-estradiol with and without MSCs in the two systems. 2 groups were implanted with the solid systems: SS-BMPβe (6 μg BMP-2 + 300 μg β-estradiol) and SS-BMPβe-MSC (6 μg BMP-2 + 300 μg β-estradiol + 5×10^5 MSCs) and 2 groups were implanted with the hydrogel system, HY-BMPβe and HY-BMPβe-MSC. The animals were sacrificed at 12 weeks post-implantation, and defect enclosing segments were resected from the calvaria.

2.7.3. ^{125}I-BMP-2 release assay

In vivo ^{125}I-BMP-2 release assay was carried out with a non-invasive method as previously described and validated [30]. This method permitted periodic assessment of the remaining ^{125}I-BMP-2 at the defect site using an external probe-type gamma counter (Captus®, Capintec Inc.). Briefly, at each sampling time point, five 1-min readings were taken at the ^{125}I emission peak (27 keV) and the mean accepted as the remaining radioactivity. The initial measure (time = 0) was considered the administered dose (100%). After 6 weeks, when no measurable levels of radioactivity remained, the rats (5 rats per group) were sacrificed.

2.8. Histology and histomorphometrical evaluation

The samples were fixed (10% formalin solution) and decalcified in Histofix® Decalcifier (Panreac) and prepared for histological analysis, as previously described [31]. New bone formation and the presence of adipose and connective tissue were identified by hematoxylin-erythrosin staining, based on their different morphological characteristics. The degree of new bone mineralization was assessed with VOF trichrome stain, in which red staining indicates advanced mineralization, whereas less mineralized, newly formed bone stains blue [32]. Sections were analysed by light microscopy (LEICA DM 4000B). Computer based image analysis software (LeicaQ-win V3 Pro-image analysis system, Barcelona, Spain) was used to evaluate histomorphometrically all sections per specimen. A region of interest (ROI) for quantitative evaluation of new bone formation and adipose and connective tissue presence, was defined as the area of the tissue within the defect. The ROI

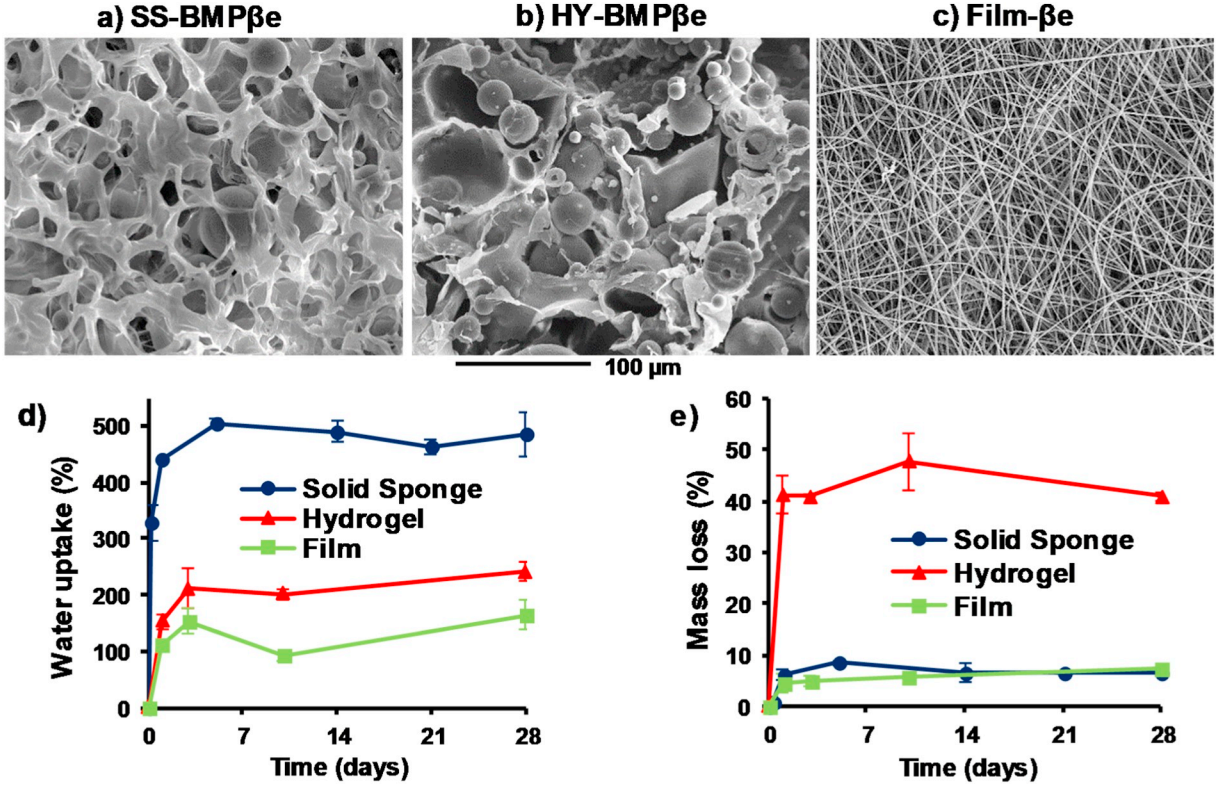

Fig. 1. Scanning electron microscope images of alginate solid sponge (a) and cross-linked hydrogel (b) containing BMP-2 and β-estradiol microspheres as well as the PLGA electrospinning film (c) containing β-estradiol. Water uptake (d) and mass loss (e) of the above systems during incubation in water at 37 °C under orbital agitation (25 rpm).

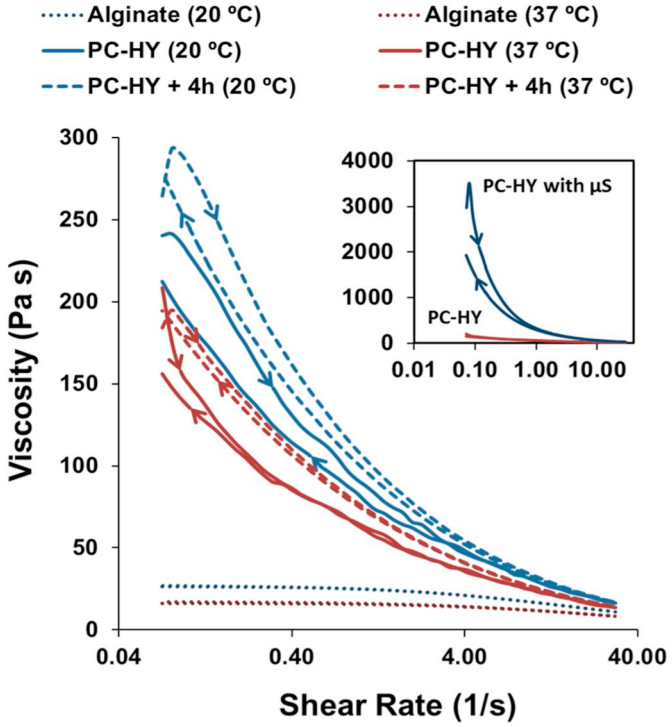

Fig. 2. Evolution of the viscosity with shear rate at 20 °C and 37 °C, of pure alginate aqueous solution (4% *w*/w) and partially cross-linked hydrogel (4% w/w alginate and 0.12% w/w of $CaCl_2$) freshly prepared (PC-HY) and after 4 h at rest (PC-HY + 4 h). In the upper right part of the figure is shown the change in viscosity of the PC-HY with the inclusion of microspheres. The curve direction (forward and backward) is indicated by arrows.

consisted of a circular region of 50 mm^2, the center of which coincided with that of the defect site. New bone formation was expressed as a percentage of repair, applying the equation,

$$\%\text{repair} = \frac{\text{new bone area}}{\text{original defect area within the ROI}} \times 100$$

Similarly, the percentage of adipose or connective tissue was obtained from the ratio between the area occupied by each specific tissue and the area of the original defect.

Statistical analyses were performed using SPSS 18.0 software. One-way analysis of variance (ANOVA) and a Tukey multiple comparison post-test were used to compare the overall performance of the different groups. Results are expressed as mean ± standard deviation. Significance was set at $p < 0.05$.

3. Results

3.1. Scaffolds characterization

The mean volume diameters of the microspheres of alginate-PLGA containing BMP-2 and PLGA microspheres with β-estradiol were 64.0 µm (10% < 14.8 µm; 90% < 111.6 µm) and 171.4 µm (10% < 46.2 µm; 90% < 286.0 µm) respectively. The encapsulation efficiency was 71% and 99% for the BMP-2 and β-estradiol, respectively.

Scaffolds were prepared by dispersing a mixture of the above microspheres in an alginate aqueous solution from which a final presentation of solid sponge or hydrogel was set. The SS scaffold presented a higher porosity (89.4 ± 1.8%) than the freeze-dried HY system (63 ± 2.2%) (Fig. 1 a, b). For in vivo administration the HY was assembled between two electrospun membranes (Fig. 1 c). The characteristics of the film were: 63.4 ± 4.3 µm of thickness, microfiber diameter of 1.2 ± 0.26 µm and 71.4 ± 4.1% of porosity (Fig. 1 c).

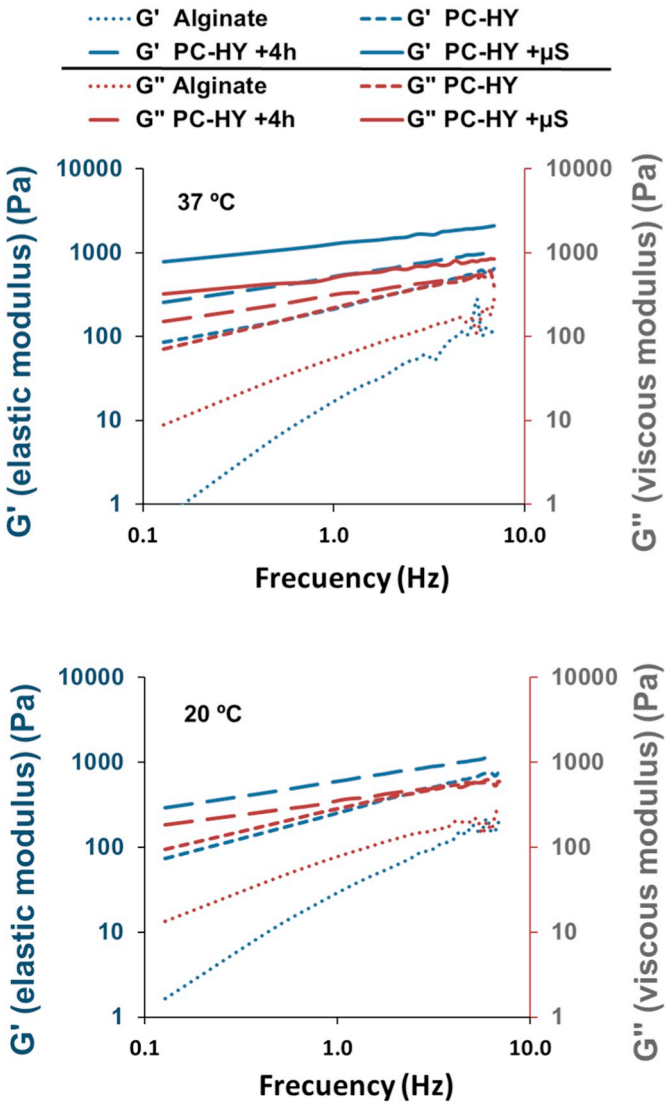

Fig. 3. Viscoelastic behaviour at 20 °C and 37 °C, of pure alginate aqueous solution (4% w/w) and partially cross-linked hydrogel (4% w/w alginate and 0.12% w/w of $CaCl_2$) freshly prepared (PC-HY) and after 4 h at rest (PC-HY + 4 h). Behaviour of PC-HY with the inclusion of microspheres (PC-HY + μS) at 37 °C is also shown.

The incubation of the systems in water at 37 °C, showed that most of the water uptake (Fig. 1 d) and mass loss (Fig. 1 e) occurred during the first days but in a different ratio depending on the system. The SS water uptake was more than double (500%) of that showed by the HY (200%) or the film (150%). On the other hand, the HY suffered a very important mass loss (40%) compared with that detected in the other two systems (6%).

3.2. Viscoelastic behaviour of hydrogel

Viscoelastic behaviour of partially cross-linked alginate hydrogel freshly prepared (PC-HY) as well as after 4 h at rest or containing microspheres were analysed.

All the samples evaluated showed a progressive viscosity decrease with the shear rate (Fig. 2), characteristic of a pseudo-plastic material. However, the viscosity curves with the increase (forward curve) and decrease (backward curve) of the shear rate in the freshly prepared PC-HY and after 4 h at rest, do not overlap, which reveals a thixotropic behaviour that was more evident at 20 °C than at 37 °C, according to a smaller hysteresis loop area recorded at this latter temperature. The

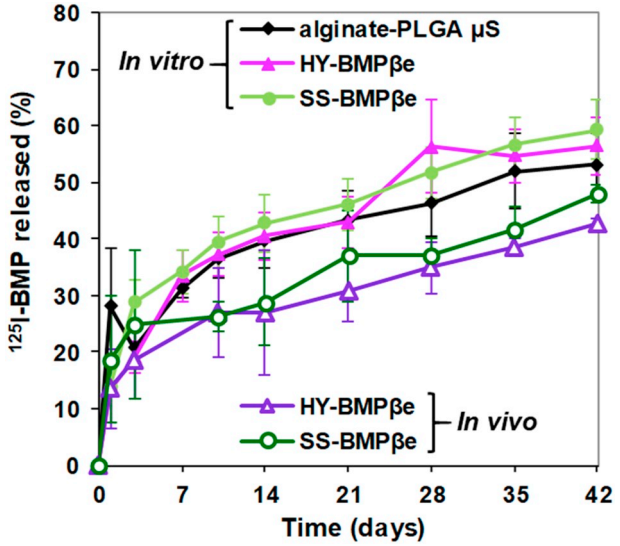

Fig. 4. BMP-2 in vitro and in vivo release assays. Release profile of ^{125}I-BMP-2 from alginate-PLGA microspheres alone and included in the hydrogel (HY-BMPβe) and solid sponge (SS-BMPβe) systems in water at 37 °C (n = 3) and after implantation in the rat calvarial defect (n = 5).

area of the hysteresis loop characterizes the energy associated with the sol-gel transition and the time for the material reorganization, hence the greater the area, the longer the time for recover its initial state after of stress [33]. The 4% *w*/w aqueous solution of alginate showed no thixotropic behaviour (Fig. 2).

The viscosity values of the freshly prepared PC-HY and after 4 h at rest or containing microspheres, were markedly superior to those of the alginate solution (4% *w*/w), especially at low shear rates (Fig. 2). In all the analysed samples, the viscosity was lower at 37 °C than at 20 °C. (Fig. 2).

For the different samples, the evolution of elastic (G′) and viscous moduli (G″) with the frequency (Fig. 3) confirms the above results. The highest G′ and G″ values were found in the PC-HY containing microspheres, followed by PC-HY after 4 h at rest and freshly prepared, the lowest values being obtained with the alginate aqueous solution (4% *w*/w). The alginate solution (4% w/w) showed a viscous behaviour, as indicated by G″ values being higher than those of G′ throughout the studied frequency range, while in PC-HY systems an evolution towards more elastic behaviour was observed. Thus, the freshly prepared PC-HY presented similar values of both G′ and G″ moduli, after 4 h at rest those values had separated resulting in an elastic module higher than the viscous module. The inclusion of the microspheres further increases this difference between the elastic and the viscous moduli due to a greater predominance of solid-like behaviour in the system.

3.3. ^{125}I-BMP-2 and β-estradiol release profiles

The in vivo release profiles of BMP-2 from SS-^{125}I-BMP and HY-^{125}I-BMP were similar, during the first 24 h approximately 20% of the dose, equivalent to 1,2 μg of the BMP-2, was released (Fig. 4). At 6 weeks, the percentage of BMP-2 released was about 43–48%. However, the in vitro ^{125}I-BMP-2 release profiles were faster than in vivo. Around 15–20% was released in the first day reaching the 57–60% released at 6 weeks. A similar in vitro release profile (Fig. 4) was obtained from the microspheres alone dispersed in the medium, which indicates that the release profile of BMP-2 from both systems, SS and HY, is governed by the microspheres.

The β-estradiol release profiles were similar in the different media used although the percentages delivered were higher (87–100%) in MeOH:water, than in the more polar media, DMSO or SLS in water, (14–25% from microspheres and 67–78% from the film) (Fig. 5).

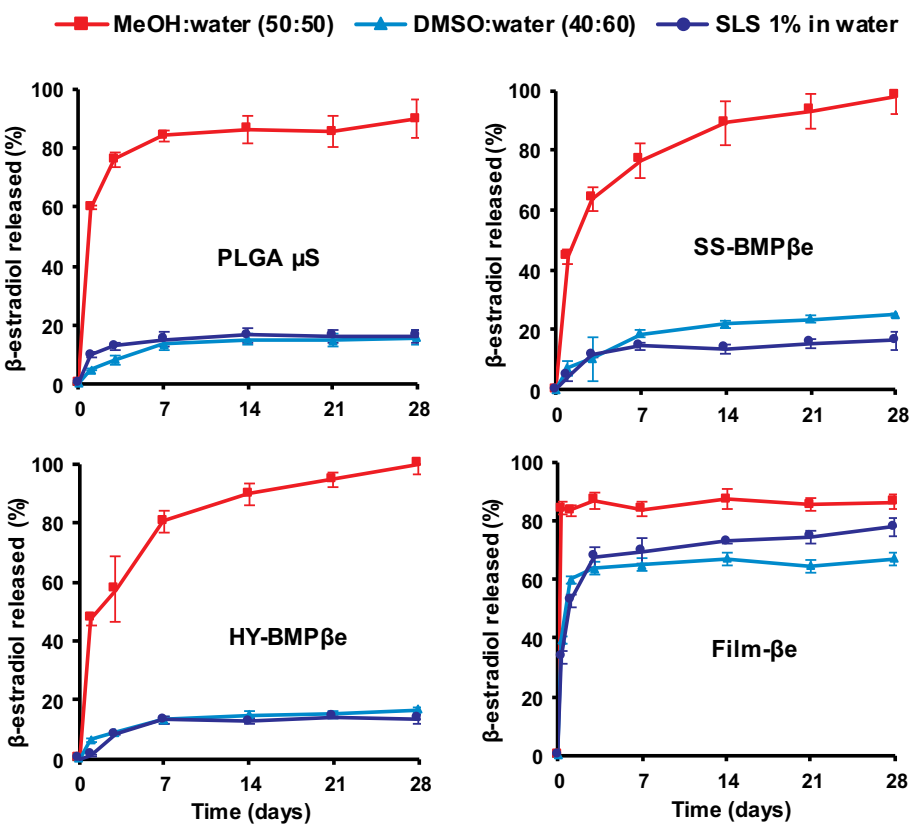

Fig. 5. Release profiles of β-estradiol from PLGA microspheres alone (PLGA μS) and included in the solid sponge (SS-BMPβe) or hydrogel (HY-BMPβe) systems as well as from the electrospinning film, at 37 °C, in three different release media: methanol:-water (50:50), dimethyl sulfoxide:water (40:60) and sodium lauryl sulphate 1% in water. (n = 3).

Therefore, the β-estradiol released was medium dependent. Regardless of medium used, β-estradiol was released faster from the films (Fig. 5 d) than from the SS and HY scaffolds (Fig. 5 b, c) being, in these last two cases, quite similar to that obtained from microspheres alone (Fig. 5 a). Thus, in MeOH:water, 84% was released in the first day from the film with no further release in the next 4 weeks while, from SS or HY, around 46% was released in the first day, reaching approximately 80% in a week and finally, almost 100% in 4 weeks. Compared with the microspheres, the β-estradiol release rate was slightly reduced during the first days by the incorporation in the SS or the HY.

3.4. Histological and histomorphometrical evaluation

Visual inspection of the SS and HY systems 12 weeks post-implantation, showed a different degree of filling of the defect, being higher in the groups implanted with the SS scaffold.

The macroscopic analysis of the calvaria showed that in groups implanted with the SS, the defect appeared completely filled with a tissue of homogeneous aspect similar to the adjacent normal bone (Fig. 6 a). This was observed both in the groups treated with BMPβe and in those treated with BMPβe + MSCs. The histological analysis confirmed the new bone formation. In all these experimental groups, the repair was observed not only in the margins but also inside the defect (Fig. 6 c, e). However, a more detailed analysis showed that the repaired bone presented a somewhat fragmented appearance, with areas of bone surrounded by connective tissue and the presence of adipose tissue between both of them (Fig. 6 g).

In the animals implanted with the HY, the macroscopic analysis of the calvaria allowed to observe clearly the morphology of the defect, filled with a tissue of semi-transparent hyaline appearance (Fig. 6 b). The histological analysis confirmed these results, the new bone formation in these animals being lower than that observed with the SS scaffold (Fig. 6 d, f). The repair in this case was mainly limited to the margins of the defect (Fig. 6 d, f). The repaired bone also showed a fragmented appearance, with a higher abundance of adipose tissue and numerous spaces of variable size that were sometimes occupied by what appeared to be remains of scaffold material (Fig. 6 h, i).

The qualitative histological results were confirmed by histomorphometrical analysis of the samples. A higher percentage of repair, between 74% in the group treated with BMPβe + MSC and 79% in that with BMPβe alone, was found in the animals implanted with the SS compared with those implanted with the HY, which ranged between 40% for the group treated with BMPβe + MSC and 50% in the group with BMPβe alone (Fig. 7 a). In fact, significant differences were found between the implanted systems, SS and HY, although no differences were observed between the applied treatments, with or without MSCs. On the other hand, in all animal groups, the proportion of mature bone, with a high degree of mineralization, was greater than the immature bone, independently of the treatment and the implanted system (Fig. 7 b). The mature bone to the immature bone ratios ranged between 1.42 and 1.67, the animals implanted with the HY presenting the lower values. Nevertheless, the statistical analysis of the data did not show significant differences neither between treatments nor between the implanted system type (Fig. 7 b).

The analysis of adipose and connective tissues in the area of the defect, revealed the existence of slightly higher amounts of adipose (22% and 17% with HY and SS respectively) than of connective tissue (18% and 10% with HY and SS respectively), being the percentages of both tissues higher with the HY systems than with the SS systems. Consequently, the ratio of adipose or connective tissue to bone present in the defect area (Fig. 7 c) were significantly higher in the HY implanted systems compared with the SS systems for both tissues. Differences due to the treatment with BMPβe or BMPβe + MSC were not found in any case.

4. Discussion

The present study evaluates the permanence time effect of BMP-2

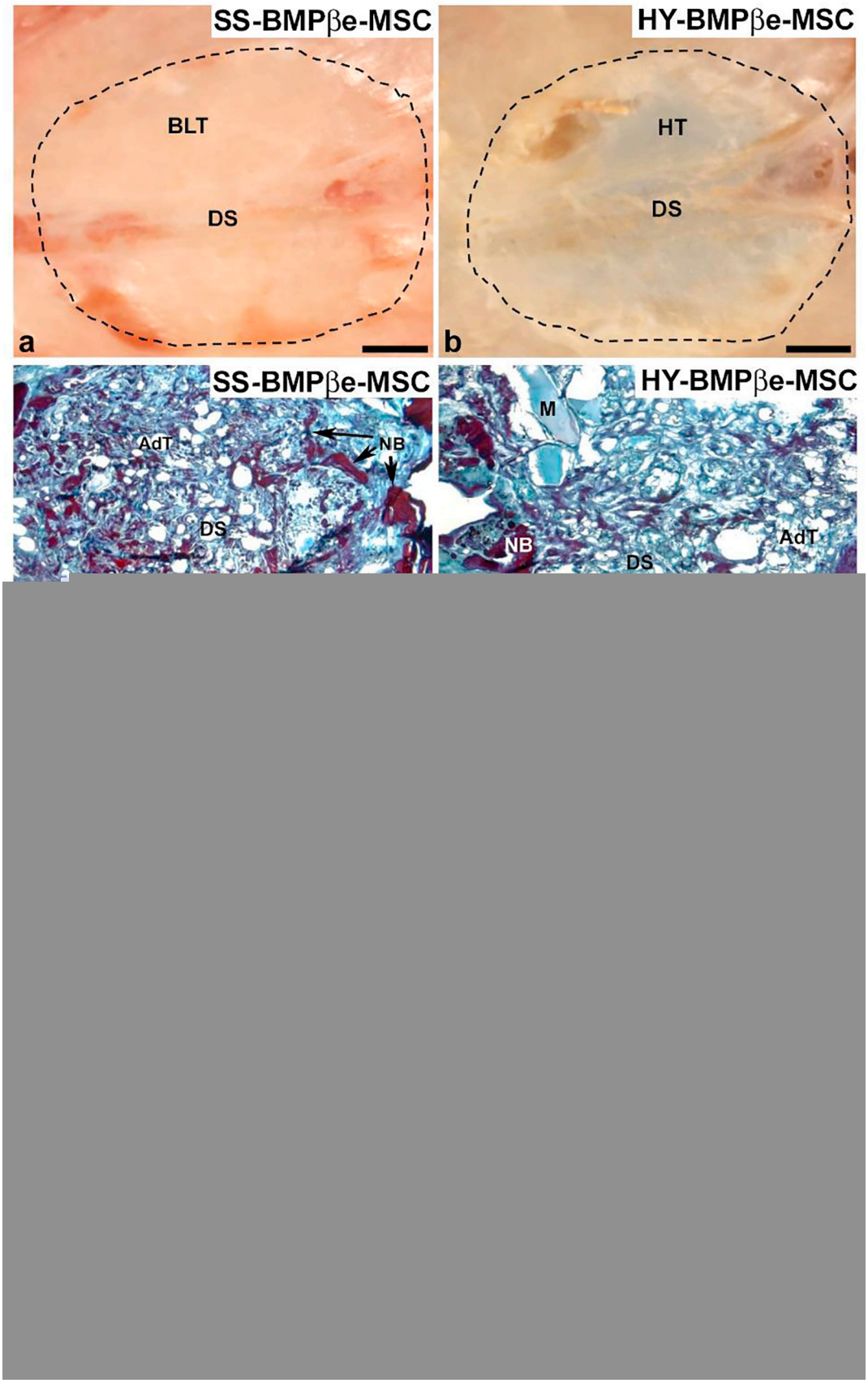

(caption on next page)

Fig. 6. Histological evaluation of the implanted systems, alginate solid sponge (SS) or in situ alginate cross-linked hydrogel (HY), containing BMP-2 and β-estradiol (BMPβe) with and without mesenchymal stem cells (MSCs) in a calvarial defect of OP rats. (a, b) macroscopic images of the defect area (dashed line) showing the extent and appearance of the repaired tissue; (c–f) microscopic images in horizontal section showing the repaired tissue (newly formed bone), as well as the presence of connective and adipose tissue in the defect area; (g, h) details at higher magnification showing the morphological characteristics of the repaired tissue with both implanted systems; (i) detail in the group HY-BMPβe showing rests of the alginate hydrogel surrounded by newly formed bone in the defect area. AdT: adipose tissue; BLT: bone like tissue; CT: connective tissue; DS: defect site; HT: hyaline tissue; M: Material; NB. New bone; sps: spaces. Scale bars = a–f: 2 mm; g: 250 μm; h: 500 μm; i: 350 μm.

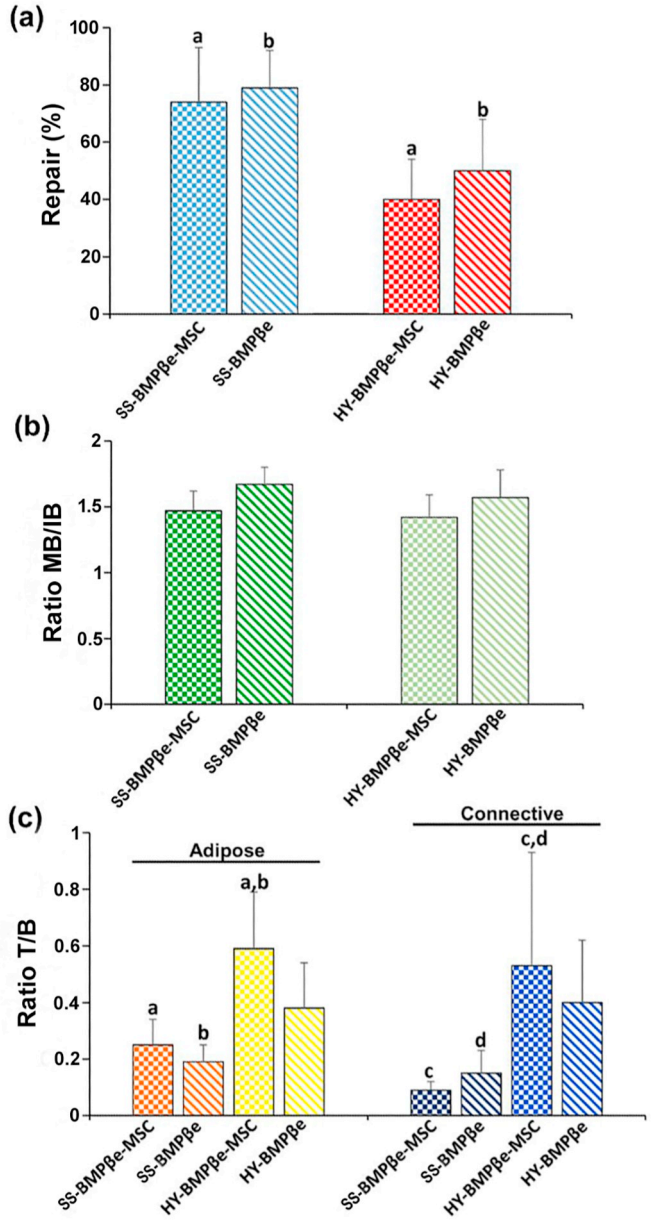

Fig. 7. Histomorphometrical evaluation of the implanted systems: (a) Degree of bone repair (%); (b) the ratio of mature bone/immature bone (MB/IB) estimated using VOF staining and (c) the ratios of adipose or connective tissue/bone (T/B) in the different experimental groups. Bars represent means ± SD ($n = 3$), $p < 0.05$. The identical letter on different bars indicates significant differences.

and β-estradiol systems with and without MSCs, in an OP rats critical size bone defect regeneration. Since bone regeneration is slower in OP animals than in non-OP, the system permanency in the defect and the maintenance of local therapeutic concentrations of BMP-2 and β-estradiol may play an important role in tissue regeneration. The material osteointegration and/or degradation rate should ideally match the bone formation rate. Therefore, the preparation of two BMP-2-β-estradiol PLGA-alginate systems, a solid sponge and a hydrogel, with the same composition, were suitable to test our hypothesis. Both systems exhibited high porosity and great water uptake capacity, these characteristics facilitate the free diffusion of oxygen and nutrients including endogenous growth factors and other cytokines providing an optimum environment for bone tissue ingrowth. Furthermore, the release profiles of both drugs from the two systems were similar as the release rate was controlled by the microspheres. In comparison with the sponge, the hydrogel had better characteristics for minimally invasive administration. Immediately after the addition of a small amount of cross-linker, the alginate solution increases its viscosity forming a dense polymer network with thixotropic behaviour, especially at 20 °C. Therefore, the viscosity of the material decreases when subjected to a certain mechanical stress, and gradually recovers at rest. This behaviour allows for the injection of highly viscous materials, even at room temperatures, and facilitate their adaptation to the target site. The incorporation of microspheres to the hydrogel increased the viscosity by 10 times while maintaining its thixotropic behaviour. To ensure formulations remain at the defect for a sufficient time, both hydrogel and sponge were placed between two electrospun polymer sheets loaded with β-estradiol forming a sandwich system. Despite of this, the hydrogel mass loss was greater than that of the sponge, hence its defect permanence time would be shorter. This characteristic probably prevents the hydrogel formulation from remaining long enough on the defect to guide tissue growth as reflected by the in vivo repair results.

Although the hydrogel formulation has the advantage of being easily injectable, sponges were also flexible and adapted perfectly to the defect edge. The histological analysis clearly showed the efficiency of the sponge system to promote bone regeneration with approximately 75% of defect regeneration against the approximately 50% reached for the hydrogel. In addition, the architecture of the repaired tissue was different, the newly formed tissue in the defects treated with the hydrogel presented a more disorganized structure with large hollow spaces, probably due to the rapid and large hydrogel mass loss observed in vitro. Additionally, a greater presence of adipose tissue, typical of osteoporosis, was found, evidencing a lower quality of the repaired tissue in this group. On the other hand, the implantation of sponges led to a more compact tissue, with a lower presence of connective tissue, probably as a consequence of the higher percentage of regeneration achieved, as this tissue plays an important role guiding and regulating the repair process at the initial steps of bone formation [34,35].

As we already reported, hydrogels of variable composition loaded with BMP-2 and β-estradiol within microsphere showed similar bone regeneration rate on calvarial defects in OP and non-OP rats. However, the mineralization process was tremendously reduced in OP rats [17,18]. For this reason, two new strategies were incorporated in the present work: the addition of MSCs and the microspheres composition modification to reduce the BMP-2 release rate. The use of polymers characterized by a relatively slow degradation rate and the incorporation of alginate in the internal aqueous phase of the microspheres was reflected in an extension of the BMP-2 release time. After 6 weeks approximately 46% of the BMP-2 dose was released in vivo. For β-estradiol, the unavailability of the radiotracer labelled molecule (that allows one to monitor the in vivo release kinetics) together with its low aqueous solubility makes difficult to predict its release profile from the implanted system. However, it is reasonable to expect the in vivo

release rate to be similar or even higher to that observed in vitro in DMSO or SLS solutions due to the continuous blood flow, which will increase as new tissue refills the defect. In any case, probably a very slow in vivo release would take place, which would be supplemented by the rapid release of the drug incorporated in the electrospun polymer sheets due to the large specific surface area of the fibers.

Unfortunately, none of the tools applied accelerated the mineralization of the formed bone. No differences were observed in the mineralization degree with either of the scaffolds with or without MSCs. The addition of MSCs to the systems pre-loaded with BMP-2 did not improve neither the regeneration rate nor the mineralization of the new bone tissue. The osteogenic effect of MSCs and BMP-2 is widely documented in the literature in different animal models. Furthermore, the synergistic effect of the combination of these two elements has been demonstrated in a calvarial defect [36–45] which is the animal model used in this study. The different animal models, composition and architecture of scaffolds, and the BMP-2 doses used by some authors together with the lack of literature (PubMed database) referred to the MSCs and BMP-2 combination efficacy for bone regeneration in osteoporosis, hinders direct comparison of our data with previous works. To the best of our knowledge, this is the first time that the combination of BMP-2 and osteoporotic MSCs has been assayed in an osteoporotic rat critical defect. The molecular alterations of osteoporotic MSCs are reflected on a proliferative capacity decrease [46], production of type I collagen-deficient matrix and a tendency to adipogenic differentiation [47] leading to significant deficiencies in self-repair and an impaired differentiation. Despite of this, the in vitro osteogenic response of osteoporotic MSCs after BMP-2 stimulation has been described [48]. Therefore, future studies are required to optimize the MSCs loading and their combination with BMP-2 to reduce the protein dose while maintaining the regenerative capacity of the system and improving the mineralization of the newly formed tissue.

5. Conclusion

In this work, two physically different PLGA-alginate scaffolds, SS and HY, have been successfully elaborated presenting the same BMP-2 and β-estradiol release rate. Both systems promoted bone regeneration in a critical size calvarial defect in OP rats, although SS showed a significantly higher percentage of bone formation. Moreover, SS promoted the formation of bone with better quality, in terms of lower proportion of adipose and connective tissue. Since the active substances release rate was similar, this difference in bone regeneration can be related to the shorter permanence time of HY in the defect and highlights the importance of the scaffold's physical configuration to optimize the effect of the sustained delivery of active molecules. Finally, the incorporation of osteoporotic MSCs in the scaffolds did not improve the bone regeneration process in any case.

Declaration of competing interest

The authors declare no conflict of interest.

Acknowledgments

This work was supported by the Ministry of Economy and Competitiveness, Spain (MAT2014-55657-R).

References

[1] H. Begam, S.K. Nandi, B. Kundu, A. Chanda, Strategies for delivering bone morphogenetic protein for bone healing, Mater. Sci. Eng. C. 70 (2017) 856–869, https://doi.org/10.1016/j.msec.2016.09.074.
[2] H.C. Fayaz, P.V. Giannoudis, M.S. Vrahas, R.M. Smith, C. Moran, H.C. Pape, C. Krettek, J.B. Jupiter, The role of stem cells in fracture healing and nonunion, Int. Orthop. 35 (2011) 1587–1597, https://doi.org/10.1007/s00264-011-1338-z.
[3] A. Nauth, B. Ristevski, R. Li, E.H. Schemitsch, Growth factors and bone regeneration: how much bone can we expect? Injury 42 (6) (2011) 574–579 (doi: 1016/j.injury.2011.03.034).
[4] D.W. Hutmacher, Scaffolds in tissue engineering bone and cartilage, Biomaterials. 21 (24) (2000) 2529–2543, https://doi.org/10.1016/s0142-9612(00)00121-6.
[5] G. Chen, N. Kawazoe, Porous scaffolds for regeneration of cartilage, bone and osteochondral tissue, Adv. Exp. Med. Biol. 1058 (2018) 171–191, https://doi.org/10.1007/978-3-319-76711-6_8.
[6] T.N. Vo, F.K. Kasper, A.G. Mikos, Strategies for controlled delivery of growth factors and cells for bone regeneration, Adv. Drug Deliv. Rev. 64 (12) (2012) 1292–1309, https://doi.org/10.1016/j.addr.2012.01.016.
[7] M.A. Velasco, C.A. Narváez-Tovar, D.A. Garzón-Alvarado, Design, materials and mechanobiology of biodegradable scaffolds for bone tissue engineering, Biomed. Res. Int. 2015 (2015) 729076, https://doi.org/10.1155/2015/729076.
[8] A.S. Hoffman, Hydrogels for biomedical applications, Adv. Drug Deliv. Rev. 64 (2012) 18–23, https://doi.org/10.1016/j.addr.2012.09.010.
[9] N.A. Peppas, J.Z. Hilt, A. Khademhosseini, R. Langer, Hydrogels in biology and medicine: from molecular principles to bionanotechnology, Adv. Mater. 18 (11) (2006) 1345–1360, https://doi.org/10.1002/adma.200501612.
[10] I.E. Bialy, W. Jiskoot, M.R. Nejadnik, Formulation, delivery and stability of bone morphogenetic proteins for effective bone regeneration, Pharm. Res. 34 (6) (2017) 1152–1170, https://doi.org/10.1007/s11095-017-2147-x.
[11] V. Agrawal, M. Sinha, A review on carrier systems for bone morphogenetic protein-2, J. Biomed. Mater. Res. Part B 105 (2016) 904–925, https://doi.org/10.1002/jbm.b.33599.
[12] P.J. Kondiah, Y.E. Choonara, P.P.D. Kondiah, T. Marimuthu, P. Kumar, L.C. du Toit, V. Pillay, A review of injectable polymeric hydrogel systems for application in bone tissue engineering, Molecules 21 (2016) E1580, , https://doi.org/10.3390/molecules21111580.
[13] M. Moreno, M.H. Amaral, J.M. Lobo, A.C. Silva, Scaffolds for bone regeneration: state of the art, Curr. Pharm. Des. 22 (2016) 2726–2736, https://doi.org/10.2174/1381612822666160203114902.
[14] R. Dorati, A. DeTrizio, T. Modena, B. Conti, F. Benazzo, G. Gastaldi, I. Genta, Biodegradable scaffolds for bone regeneration combined with drug-delivery systems in osteomyelitis therapy, Pharmaceuticals 10 (2017) E96, , https://doi.org/10.3390/ph10040096.
[15] M. Rodríguez-Évora, R. Reyes, C. Alvarez-Lorenzo, A. Concheiro, A. Delgado, C. Évora, Bone regeneration induced by an in situ gel-forming poloxamine, bone morphogenetic protein-2 system, J. Biomed. Nanotechnol. 10 (2014) 1–11, https://doi.org/10.1166/jbn.2014.1801.
[16] C. del Rosario, M. Rodríguez-Évora, R. Reyes, S. Simões, A. Concheiro, C. Évora, C. Alvarez-Lorenzo, A. Delgado, Bone critical defect repair with poloxamine-cyclodextrin supramolecular gels, Int. J. Pharm. 495 (2015) 463–473, https://doi.org/10.1016/j.ijpharm.2015.09.003.
[17] E. Segredo-Morales, R. Reyes, M.R. Arnau, A. Delgado, C. Évora, In situ gel-forming system for dual BMP-2 and 17β-estradiol controlled release for bone regeneration in osteoporotic rats, Drug Deliv. Transl. Res. 8 (2018) 1103–1113, https://doi.org/10.1007/s13346-018-0574-9.
[18] E. Segredo-Morales, P. García-García, R. Reyes, E. Pérez-Herrero, A. Delgado, C. Évora, Bone regeneration in osteoporosis by delivery BMP-2 and PRGF from tetronic–alginate composite thermogel, Int. J. Pharm. 543 (2018) 160–168, https://doi.org/10.1016/j.ijpharm.2018.03.034.
[19] T. Kubo, T. Shiga, J. Hashimoto, M. Yoshioka, H. Honjo, M. Urabe, I. Kitajima, I. Semba, Y. Hirasawa, Osteoporosis influences the late period of fracture healing in a rat model prepared by ovariectomy and low calcium diet, J. Steroid Biochem. Mol. Biol. 68 (1999) 197–202, https://doi.org/10.1016/S0960-0760(99)00032-1.
[20] H. Namkung-Matthai, R. Appleyard, J. Jansen, J. Hao Lin, S. Maastricht, M. Swain, R.S. Mason, G.A. Murrell, A.D. Diwan, T. Diamond, Osteoporosis influences the early period of fracture healing in a rat osteoporotic model, Bone 28 (2001) 80–86, https://doi.org/10.1016/S8756-3282(00)00414-2.
[21] R. Oliver, Y. Yu, G. Yee, A. Low, A. Diwan, W. Walsh, Poor histological healing of a femoral fracture following 12 months of oestrogen deficiency in rats, Osteoporos. Int. 24 (2013) 2581–2589, https://doi.org/10.1007/s00198-013-2345-2.
[22] W.H. Cheung, T. Miclau, S.K. Chow, F.F. Yang, V. Alt, Fracture healing in osteoporotic bone, Injury Int. J. Care Injured 47 (S2) (2016) 21–26, https://doi.org/10.1016/S0020-1383(16)47004-X.
[23] G. Gainza, J.J. Aguirre, J.L. Pedraz, R.M. Hernández, M. Igartua, rhEGF-loaded PLGA-alginate microspheres enhance the healing of full-thickness excisional wounds in diabetised Wistar rats, Eur. J. Pharm. Sci. 50 (2013) 243–252, https://doi.org/10.1016/j.ejps.2013.07.003.
[24] P. Zhai, X.B. Chenb, D.J. Schreyer, PLGA/alginate composite microspheres for hydrophilic protein delivery, Mater. Sci. Eng. C Mater. Biol. Appl. 56 (2015) 251–259, https://doi.org/10.1016/j.msec.2015.06.015.
[25] P.J. Fraker, J.C. Speck Jr., Protein and cell membrane iodinations with a sparingly soluble chloroamide, 1,3,4,6-tetrachloro-3a,6a-diphrenylglycoluril, Biochem. Biophys. Res. Commun. 80 (1978) 849–857, https://doi.org/10.1016/0006-291x(78)91322-0.
[26] K.R. Dobson, L. Reading, M. Haberey, X. Marine, A. Scutt, Centrifugal isolation of bone marrow from bone: an improved method for the recovery and quantitation of bone marrow osteoprogenitor cells from rat tibiae and femurae, Calcif. Tissue Int. 65 (1999) 411–413, https://doi.org/10.1007/s002239900723.
[27] R. Reyes, M.K. Pec, E. Sánchez, C. del Rosario, A. Delgado, C. Évora, Comparative, osteochondral defect repair: stem cells versus chondrocytes versus bone morphogenetic protein-2, solely or in combination, Eur. Cell. Mater. 25 (2013) 351–365, https://doi.org/10.22203/eCM.v025a25.
[28] R. Vayas, R. Reyes, M.R. Arnau, C. Évora, A. Delgado, Injectable scaffold for bone marrow stem cells and bone morphogenetic protein-2 to repair cartilage, Cartilage

(2019) 1–14, https://doi.org/10.1177/1947603519841682.
[29] M. Rodríguez-Évora, A. Delgado, R. Reyes, A. Hernández-Daranas, I. Soriano, J. San Román, C. Évora, Osteogenic effect of local, long versus short term BMP-2 delivery from a novel SPU-PLGA-βTCP concentric system in a critical size defect in rats, Eur. J. Pharm. Sci. 49 (2013) 873–884, https://doi.org/10.1016/j.ejps.2013.06.008.
[30] J.J. Delgado, C. Evora, E. Sánchez, M. Baro, A. Delgado, Validation of a method for non-invasive in vivo measurement of growth factor release from a local delivery system in bone, J. Control. Release 114 (2006) 223–229, https://doi.org/10.1016/j.jconrel.2006.05.026.
[31] A. Hernández, E. Sánchez, I. Soriano, R. Reyes, A. Delgado, C. Évora, Material-related effects of BMP-2 delivery systems on bone regeneration, Acta Biomater. 8 (2012) 781–791, https://doi.org/10.1016/j.actbio.2011.10.008.
[32] E. Martinez-Sanz, D.A. Ossipov, J. Hilborn, S. Larsson, K.B. Jonsson, O.P. Varghese, Bone reservoir: injectable hyaluronic acid hydrogel for minimal invasive bone augmentation, J. Control. Release 152 (2011) 232–240, https://doi.org/10.1016/j.jconrel.2011.02.003.
[33] R. Barbucci, D. Pasqui, R. Favaloro, G. Panariello, Thixotropic hydrogel from chemically cross-linked guar gum: synthesis, characterization and rheological behaviour, Carbohydr. Res. 343 (2008) 3058–3065, https://doi.org/10.1016/j.carres.2008.08.029.
[34] J.M. Reinke, H. Sorg, Wound repair and regeneration, Eur. Surg. Res. 49 (2012) 35–43, https://doi.org/10.1159/000339613.
[35] E.S. Chermnykh, E.V. Kiseleva, O.S. Rogovaya, A.L. Rippa, A.V. Vasiliev, E.A. Vorotelyak, Tissue-engineered biological dressing accelerates skin wound healing in mice via formation of provisional connective tissue, Histol. Histopathol. 33 (2018) 1189–1199, https://doi.org/10.14670/HH-18-006.
[36] S.J. Stephan, S.S. Tholpady, B. Gross, C.E. Petrie-Aronin, E.A. Botchway, L.S. Nair, R.C. Ogle, S.S. Park, Inyectable tissue-engineered bone repair of a rat calvarial defect, Laryngoscope. 120 (2010) 895–901, https://doi.org/10.1002/lary.20624.
[37] X. He, Y. Liu, X. Yuan, L. Lu, Enhanced healing of rat calvarial defects with MSCs loaded on BMP-2 releasing chitosan/alginate/hidroxyapatite scaffolds, PLoS One 9 (2014) e104061, , https://doi.org/10.1371/journal.pone.0104061.
[38] C. del Rosario, M. Rodríguez-Évora, R. Reyes, A. Delgado, C. Évora, BMP-2, PDGF-BB, and bone marrow mesenchymal cells in a macroporous β-TCP scaffold for critical-size bone defect repair in rats, Biomed. Mater. 10 (2015) 045008, , https://doi.org/10.1088/1748-6041/10/4/045008.
[39] B.S. Kim, M.K. Choi, J.H. Yoon, J. Lee, Evaluation of bone regeneration with biphasic calcium phosphate substitute implanted with bone morphogenetic protein 2 and mesenchymal stem cells in a rabbit calvarial defect model, Oral Surg. Oral Med. Oral Pathol. Oral Radiol. 120 (1) (2015) 2–9, https://doi.org/10.1016/j.oooo.2015.02.017.
[40] S. Eap, L. Keller, J. Schiavi, O. Huck, L. Jacomine, F. Fioretti, C. Gauthier, V. Sebastian, P. Schwinté, N. Benkirane-Jessel, A living thick nanofibrous implant bifunctionalized wht active growth factor and stem cells for bone regeneration, Int. J. Nanomedicine 10 (2015) 1061–1075, https://doi.org/10.2147/IJN.S72670.
[41] S.S. Ho, N.L. Vollmer, M.I. Refaat, O. Jeon, E. Alsber, M.A. Lee, J.K. Leach, Bone morphogenetic protein-2 promotes human mesenchymal stem cell survival and resultant bone formation when entrapped in photocrosslinked alginate hydrogels, Adv. Healthc. Mater. 5 (2016) 2501–2509, https://doi.org/10.1002/adhm.201600461.
[42] R. Aquino-Martínezx, N. Artigas, B. Gámez, J.L. Rosa, F. Ventura, Extracellular calcium promotes bone formation from bone marrow mesenchymal stem cells by amplifying the effects of BMP-2 on SMAD signalling, PLoS One 12 (2017) e0178158, , https://doi.org/10.1371/journal.pone.0178158.
[43] R. Zhang, X. Li, Y. Liu, X. Gao, T. Zhu, L. Lu, Acceleration of bone regeneration in critical-size defect using BMP-9-loaded nHA/Coll/MWCNTs scaffolds seeded with bone marrow mesenchymal stem cells, Biomed. Res. Int. 2019 (2019) 7343957, , https://doi.org/10.1155/2019/7343957.
[44] X. Li, R. Zhang, X. Tan, B. Li, Y. Liu, X. Wang, Synthesis and evaluation of BMMSC-seeded BMP-6/nHAG/GMS scaffolds for bone regeneration, Int. J. Med. Sci. 16 (2019) 1007–1017, https://doi.org/10.7150/ijms.31966.
[45] Y. Kong, Y. Zhao, D. Li, H. Shen, M. Yan, Dual delivery of encapsulated BM-MSCs and BMP-2 improves osteogenic differentiation and new bone formation, J. Biomed. Mater. Res. A 107 (2019) 2282–2295, https://doi.org/10.1002/jbm.a.36737.
[46] E. Tsiridis, N. Upadhyay, P. Giannoudis, Molecular aspects of fracture healing: which are the important molecules? Injury 38 (2007) S11–S25, https://doi.org/10.1016/j.injury.2007.02.006.
[47] J.P. Rodríguez, L. Montecinos, S. Ríos, P. Reyes, J. Martínez, Mesenchymal stem cells from osteoporotic patients produce a type I collagen-deficient extracellular matrix favoring adipogenic differentiation, J. Cell. Biochem. 79 (2000) 557–565, https://doi.org/10.1002/1097-4644(20001215)79:4<557::AID-JCB40>3.0.CO;2-H.
[48] W.C. Prall, F. Haasters, J. Heggebö, H. Polzer, C. Schwarz, C. Gassner, S. Grote, D. Anz, M. Jäger, W. Mutschler, M. Schieker, Mesenchymal stem cells from osteoporotic patients feature impaired signal transduction but sustained osteoinduction in response to BMP-2 stimulation, Biochem. Biophys. Res. Commun. 440 (2013) 617–622, https://doi.org/10.1016/j.bbrc.2013.09.114.